Ch.8: Polarons in p-conjugated semiconductors: absorption spectroscopy and spin-dependent recombination

M. Wohlgenannt, phys. stat. sol. (a) **201**, 1188–1204 (2004)

2009. 4. 21.

Changhee Lee
School of Electrical Engineering and Computer Science
Seoul National Univ.
chlee7@snu.ac.kr

Polaron in organic semiconductors

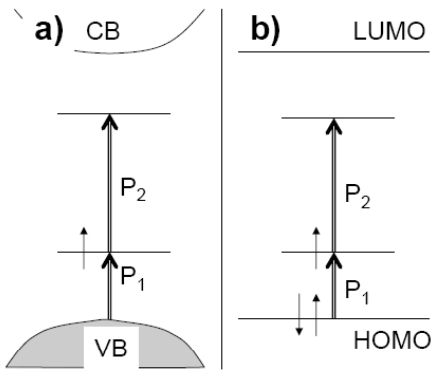

Comparison between different models for the positive polaron:
a) Electron–phonon (SSH) model.
b) Molecular orbital picture.

M. Wohlgenannt, phys. stat. sol. (a) **201**, 1188–1204 (2004)

PA spectra of π-conjugated materials

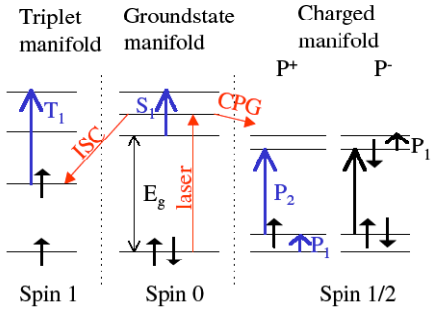

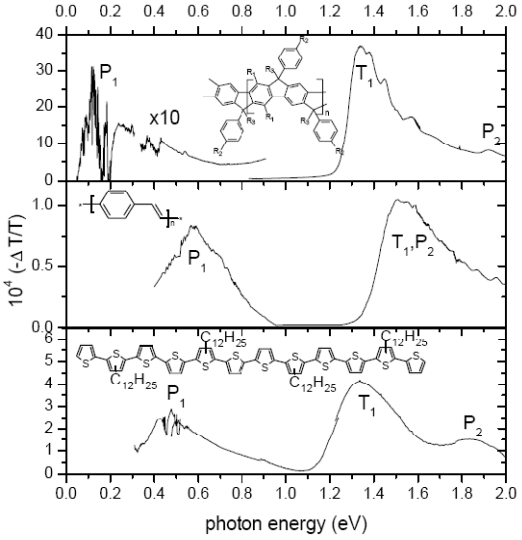

M. Wohlgenannt, phys. stat. sol. (a) **201**, 1188–1204 (2004)

P_1 polaron transition in a variety of oligomers

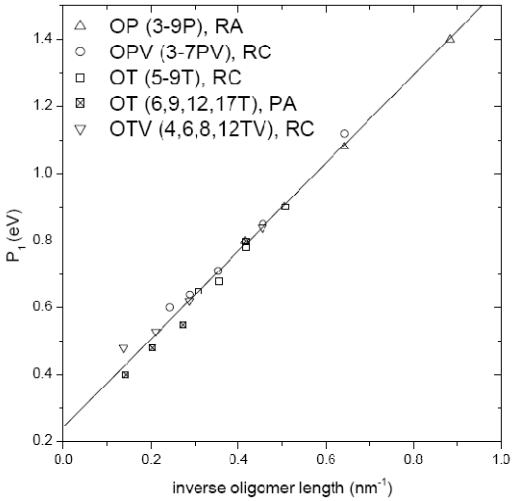

M. Wohlgenannt, phys. stat. sol. (a) **201**, 1188–1204 (2004)

P_1 polaron transition in polyene oligomers

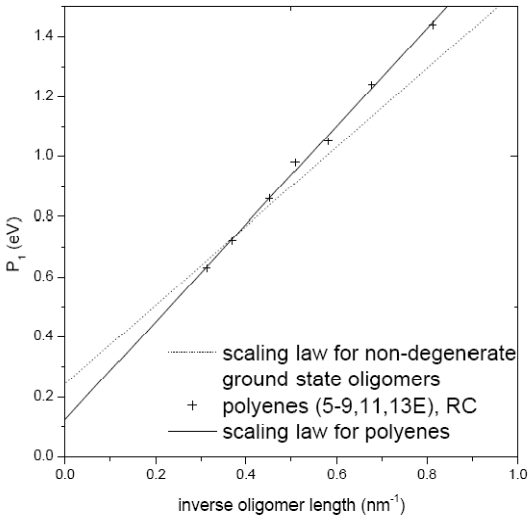

M. Wohlgenannt, phys. stat. sol. (a) **201**, 1188–1204 (2004)

P_1 polaron transition in π-conjugated polymer films

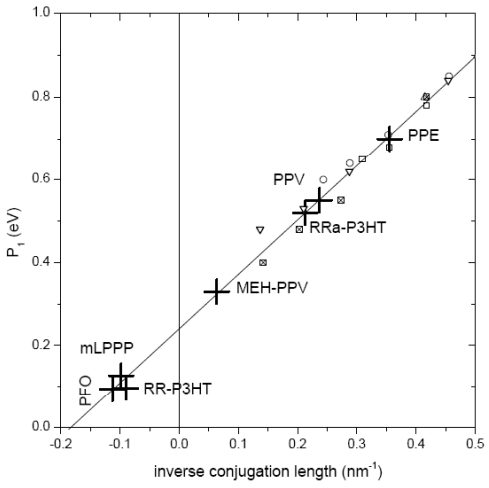

For mLPPP, RR-P3HT, and PFO, $P_1 < P_{1\infty}$ which is indicative of a destabilization of the polaron as a result of interchain interactions.

M. Wohlgenannt, phys. stat. sol. (a) **201**, 1188–1204 (2004)

Is polaron recombination (exciton formation) spin-dependent?

EL Efficiency in PLED

Y. Cao, I. D. Parker, G. Yu, C. Zhang, UNIAX, Nature **397**, 414 (1999)

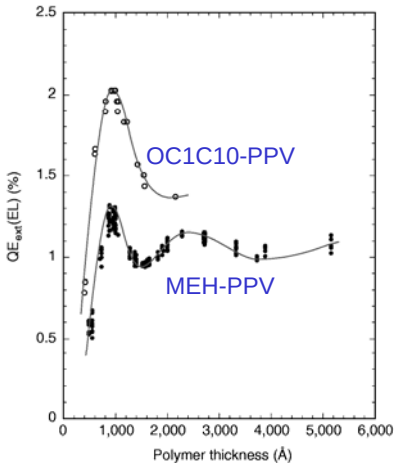

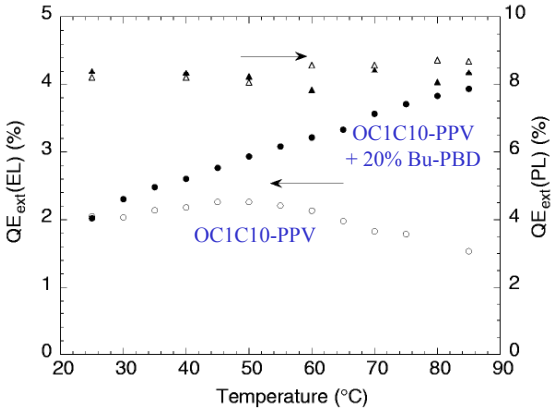

* EL efficiency > 50% of PL efficiency

Exciton formation

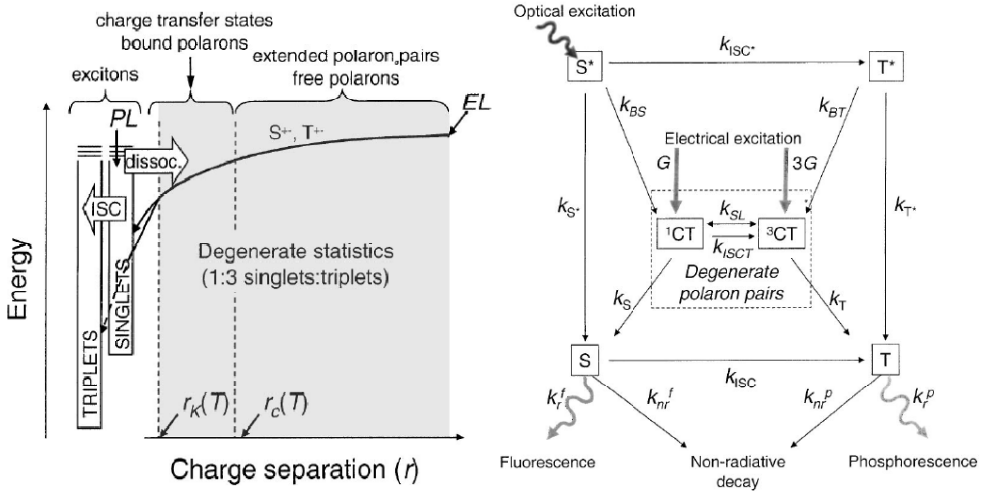

M. Segel, M. A. Baldo, R. J. Holmes, S. R. Forrest, Z. G. Soos, Phys. Rev. B 68, 075211 (2003)

PADMR of 12T

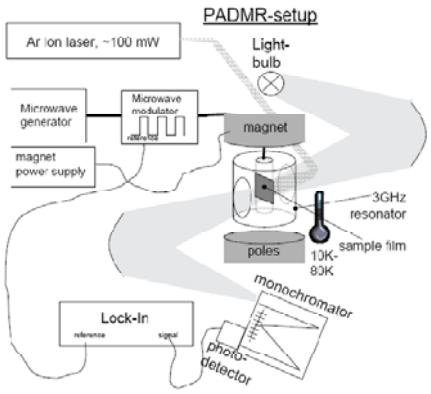

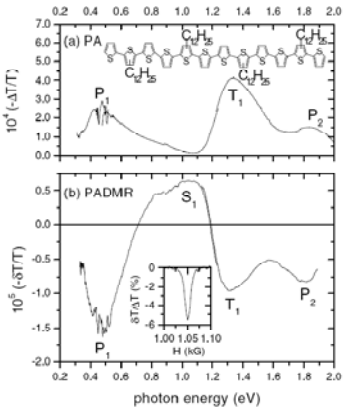

Fig. 10 a) The PA spectrum of 12 T (inset); (b) the PADMR spectrum at magnetic field $H = 1.05$ kG corresponding to $S = 1/2$ resonance (see inset in (b)). Both spectra (a) and (b) show two bands (P_1 and P_2) due to polarons, T_1 is due to triplet absorption. S_1 is assigned to singlets. The PA was measured at 80 K, excitation by the 488 nm Ar^+ laser line (500 mW); the PADMR spectrum was measured at 10 K.

• The spin 1/2 PADMR spectrum shows a negative magnetic resonance response at the T_1 triplet exciton PA band, in addition to P_1 and P_2 PADMR bands. → Polarons can recombine to form triplet excitons. Since the polaron population is reduced by spin-1/2 resonance, then spin-1/2 resonance indirectly affects the triplet population via the exciton formation process.

• The observation of a negative T_1 spin-1/2 magnetic resonance indicates that the polaron recombination process is bimolecular and non-geminate in nature.

M. Wohlgenannt, phys. stat. sol. (a) **201**, 1188–1204 (2004)

PADMR of PPV

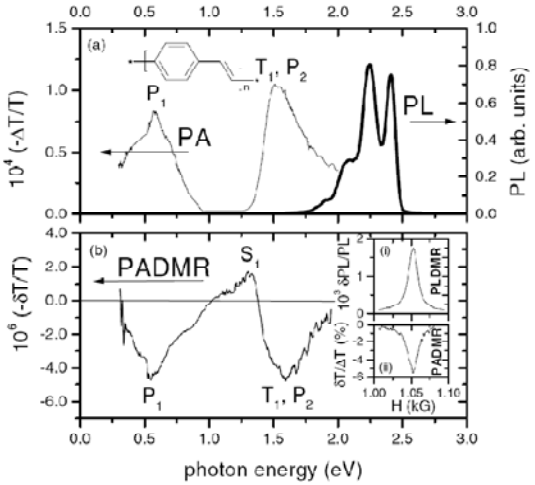

Fig. 11 a) The PA and PL spectra of PPV (see inset); (b) the PADMR spectrum at magnetic field H = 1.05 kG that corresponds to S = 1/2 resonance. Inset (i) shows the spin 1/2 PLDMR resonance, whereas inset (ii) shows spin-1/2 PADMR resonance. Both spectra (a) and (b) show two main bands (P_1 and (T_1, P_2) (see text)). P_1 and P_2 are due to polarons, T_1 is due to triplet absorption. The positive PADMR band S_1 is assigned to singlet absorption in agreement with the positive H-PLDMR response (see inset (i) in (b)). The PA and PL (PADMR and PLDMR) were measured at 80 K (10 K), excitation was 457 nm Ar^+ laser line (300 mW), modulated at 1 kHz.

Polarons can recombine to form singlet excitons, and therefore spin-1/2 resonance indirectly influences the singlet population via the exciton formation process. A reduction in polaron density would then lead to a reduction in singlet-polaron quenching and therefore an increase in singlets.

M. Wohlgenannt, phys. stat. sol. (a) **201**, 1188–1204 (2004)

Dependencies of PL, δPL and polaron PA band P_1 on the laser intensity in a PPV film.

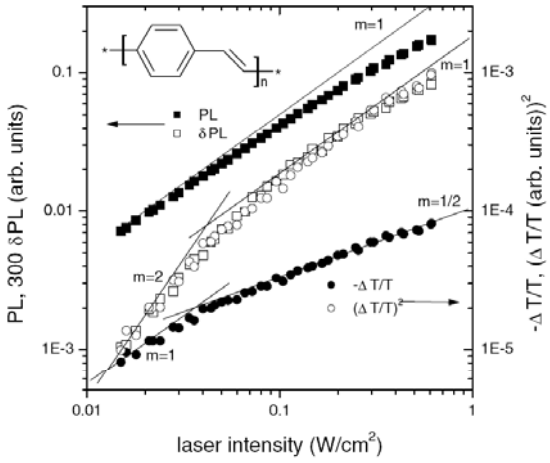

Fig. 12 The laser intensity dependencies of the photoluminescence (PL, solid squares), the magnetic resonance effect on the photoluminescence (δ PL, open squares), the polaron PA band measured at 0.55 eV ($-\Delta T/T$, solid circle) and its square (open circles, rescaled) in a PPV film measured at 10 K. The modulation frequency was 1 kHz.

Polaron recombination follows a rate equation law with bimolecular recombination kinetics:

$$\frac{dN}{dt} = \eta\Phi - BN^2$$

M. Wohlgenannt, phys. stat. sol. (a) **201**, 1188–1204 (2004)

$\sigma_S > \sigma_T$?

Origin of the PLDMR and that polaron recombination is non-geminate.

→ Positive singlet signal and a negative triplet signal show that $\sigma_S > \sigma_T$.

Magnetic resonance leads to a randomization of the spin-alignment of the recombining pairs of polarons. At all times, the four possible spin states of the recombining polarons are equally populated, and each pair of polarons changes its spin state rapidly on the time scale of recombination. This then leads to continuous competition between singlet and triplet formation. Therefore more efficient channel leads to a positive signal, whereas the less efficient channel leads to a negative signal.

M. Wohlgenannt, phys. stat. sol. (a) **201**, 1188–1204 (2004)

Reaction rate of spin parallel and perpendicular pairs

$|P^+> + |P^-> \rightarrow |S> + |G>$
$|T> + |G>$

Spin ½ + ½ = 0 (Singlet), 1 (Triplet)

Singlet
spin anti-symmetric

$$|\chi_1\chi_2> = \frac{1}{\sqrt{2}}|\uparrow\downarrow> - |\downarrow\uparrow>$$ } anti-parallel spin

$$|\chi_1\chi_2> = \frac{1}{\sqrt{2}}|\uparrow\downarrow> + |\downarrow\uparrow>$$

Triplet
spin symmetric

$$|\chi_1\chi_2> = |\uparrow\uparrow>$$
$$|\chi_1\chi_2> = |\downarrow\downarrow>$$ } parallel spin

Reaction rate between spin parallel pairs: $R_P \propto 2\sigma_T$

Reaction rate between spin antiparallel pairs: $R_{AP} \propto (\sigma_S + \sigma_T)$

$$\delta N/N = -(R_P - R_{AP})^2/(R_P + R_{AP})^2 \propto \delta T/T$$

Spin-dependent recombination spectroscopy

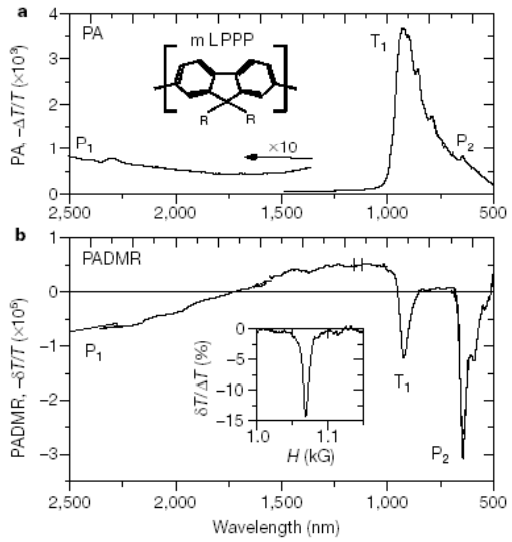

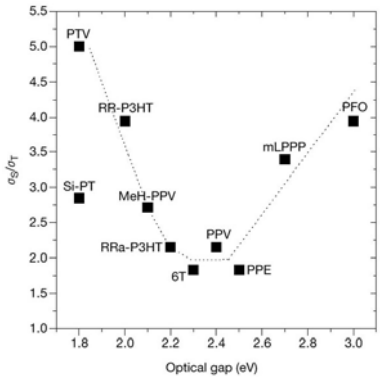

$$\frac{\sigma_S}{\sigma_T} = \frac{1+3\left|\delta T/\Delta T\right|^{1/2}}{1-\left|\delta T/\Delta T\right|^{1/2}}$$

δT: PADMR signal
ΔT: PA signal

Conjugation length dependence of Spin Dependent Exciton Formation

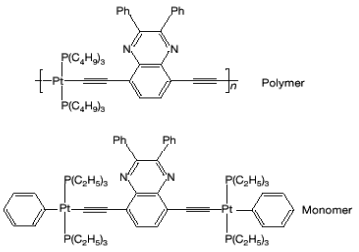

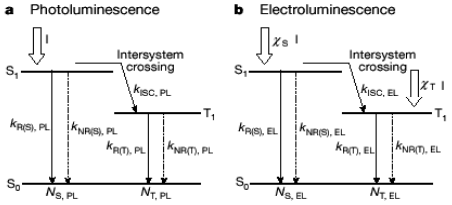

R. For photoluminescence:

$$N_{S,PL} = I\Phi_{SR,PL}$$

$$N_{T,PL} = I\Phi_{ISC,PL}\Phi_{TR,PL}$$

$$R_{PL} = \frac{N_{T,PL}}{N_{S,PL}} = \frac{\Phi_{ISC,PL}\Phi_{TR,PL}}{\Phi_{SR,PL}}$$

For electroluminescence:

$$N_{S,EL} = I\chi_S\Phi_{SR,EL}$$

$$N_{T,EL} = I\chi_S\Phi_{ISC,EL}\Phi_{TR,EL} + I\chi_T\Phi_{TR,EL}$$

$$R_{EL} = \frac{N_{T,EL}}{N_{S,EL}} = \frac{\chi_S\Phi_{ISC,EL}\Phi_{TR,EL} + \chi_T\Phi_{TR,EL}}{\chi_S\Phi_{SR,EL}}$$

Comparing photoluminescence and electroluminescence gives:

$$\frac{R_{PL}}{R_{EL}} = \left(\frac{\chi_S\Phi_{ISC,PL}}{\chi_S\Phi_{ISC,EL} + \chi_T}\right)\left(\frac{\Phi_{TR,PL}}{\Phi_{TR,EL}}\right)\left(\frac{\Phi_{SR,EL}}{\Phi_{SR,PL}}\right) \quad (1)$$

$$\frac{R_{PL}}{R_{EL}} = \left(\frac{\chi_S\Phi_{ISC,PL}}{\chi_S\Phi_{ISC,EL} + (1-\chi_S)}\right) \quad (2)$$

For these materials Φ_{ISC} is known to be close to one[8] so we approximate equation (2) by:

$$\frac{R_{PL}}{R_{EL}} = \chi_S \quad (3)$$

J. S. Wilson, A. S. Dhoot, A. J. A. B. Seeley, M. S. Khan, A. Kohler, R. H. Friend, Nature **413**, 828 (2001)

Conjugation length dependence of Spin Dependent Exciton Formation

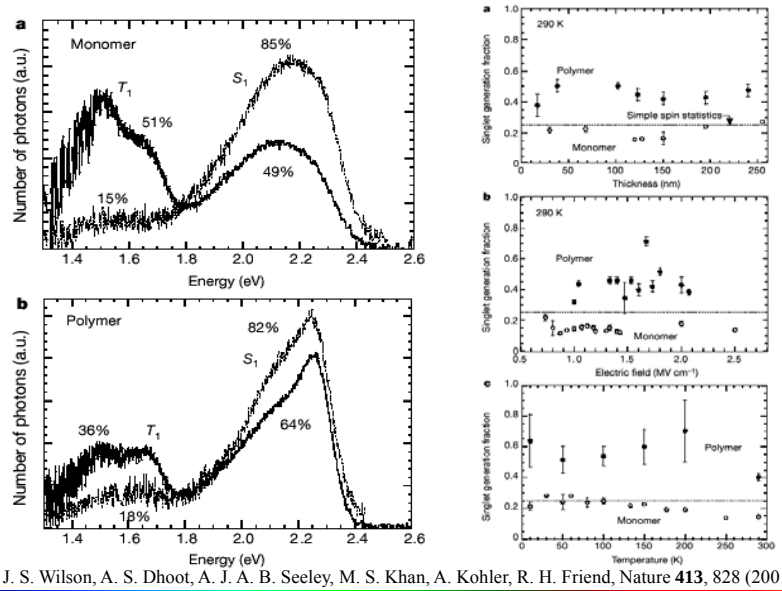

J. S. Wilson, A. S. Dhoot, A. J. A. B. Seeley, M. S. Khan, A. Kohler, R. H. Friend, Nature **413**, 828 (2001)

Carrier Recombination

Interchain or Intermolecular Hopping

Recombination of injected *e* and *h*

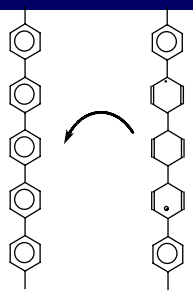

D. Beljonne et al., Adv. Funct. Mater. 14, 684 (2004)

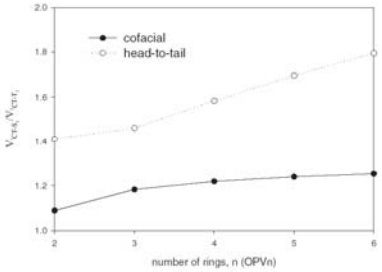

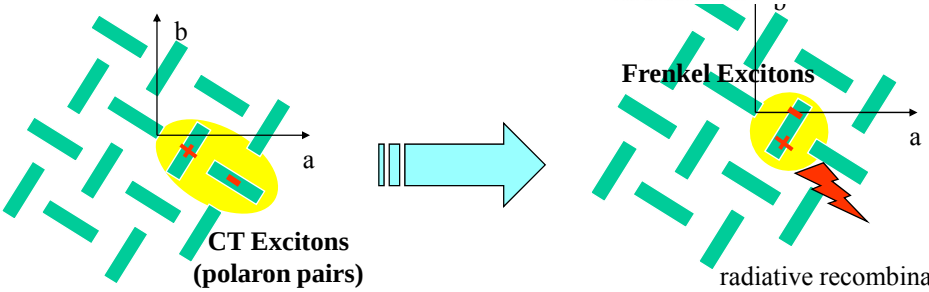

Experimental setup

$$P_{PL} = \eta_C h\nu \frac{k_R}{k_R + k_{NR} + k_Q}\phi \qquad \Delta P_{PL} = P_{PL}(k_Q) - P_{PL}(k_Q = 0) \approx -h\nu\,\eta_C \eta_{PL} \frac{k_Q}{k_R + k_{NR}}\phi \qquad \eta_{PL} = k_R/(k_R + k_{NR})$$

$$I_{ph} = q\frac{k_Q}{k_R + k_{NR} + k_Q}\phi \qquad \eta_C \eta_{PL} = -\frac{q}{h\nu}\frac{\Delta P_{PL}}{I_{ph}}$$

$$\eta_{EL} = \chi_S \gamma\, \eta_C \eta_{PL} \qquad P_{EL} = qI_{inj} h\nu \eta_{EL}$$

$$\chi_S \gamma = \frac{\eta_{EL}}{\eta_C \eta_{PL}} = \frac{P_{EL}}{I_{inj}} \Big/ \frac{-\Delta P_{PL}}{I_{ph}}$$

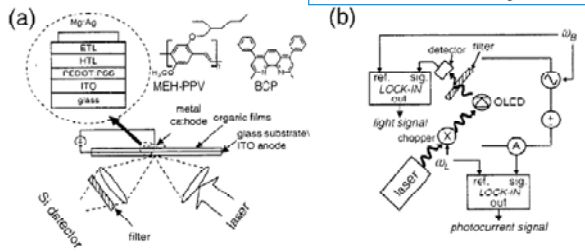

FIG. 3. (a) The experimental setup of the dc PL efficiency measurement. PL from an optically excited OLED is focused onto a calibrated silicon detector. An optical filter is used to remove the pump light from the collected light. The OLED is placed under a varying reverse bias that partially quenches the PL. The out-coupled PL efficiency is obtained by comparing the change in PL (ΔP_{PL}) to the photocurrent. Inset: A cross section of the OLED's. Charges and excitons within the organic layer under test are confined by a heterostructure employing bathocuproine (BCP) as the electron transport (ETL) and hole blocking layer. The semiconducting polymer MEH-PPV was used as a hole transport layer (HTL). (b) The experimental setup of the synchronous PL efficiency measurement. Here the photocurrent and out-coupled PL are detected by locking the photocurrent to the optical chopping frequency, and the PL to the modulation frequency of the reverse bias voltage. This scheme rejects leakage current, optical pump fluctuation, and detected light noise.

M. Segal, M. A. Baldo, R. J. Holmes, S. R. Forrest, Z. G. Soos, Phys. Rev. B 68, 075211 (2003).

Excitonic S/T ratios in molecular and polymeric organic materials

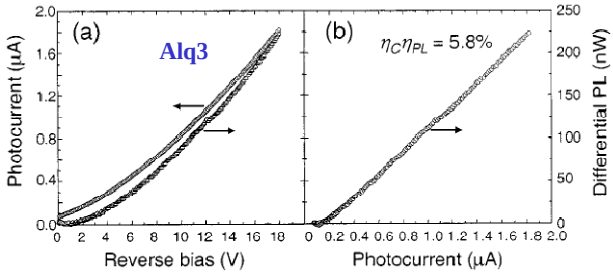

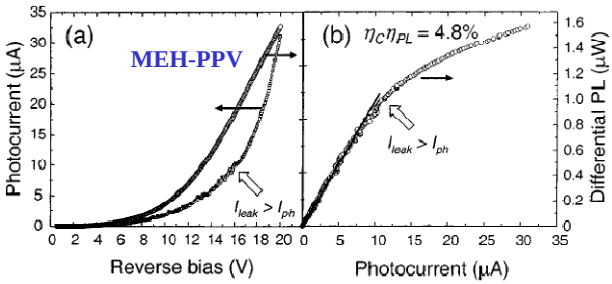

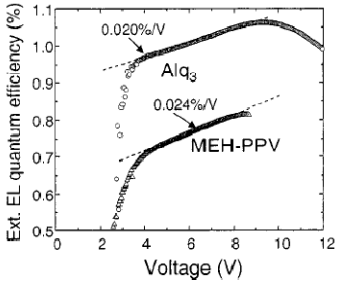

$$\chi_S \gamma = \frac{\eta_{EL}}{\eta_C \eta_{PL}} = \frac{P_{EL}}{I_{inj}} \Big/ \frac{-\Delta P_{PL}}{I_{ph}}$$

$\chi_S\gamma$=(18.0±0.3)% for Alq3
$\chi_S\gamma$=(17.0±0.7)% for MEH-PPV

M. Segal, M. A. Baldo, R. J. Holmes, S. R. Forrest, Z. G. Soos, Phys. Rev. B 68, 075211 (2003).

Excitonic S/T ratios in molecular and polymeric organic materials

TABLE I. Summary of various measurements of χ_s using EL/PL comparisons.

(a) Small molecular weight materials

(i) Direct comparisons of EL to PL

Material	η, η_{PL} (%)	η_{EL} (%)	γ	χ_s	Ref.
Alq_3[a]	5.8	1.06	0.91 ± 0.05	0.20 ± 0.01	

(ii) Phosphorescent techniques

Material	η^f_{PL}/η^p_{PL}	η^f_{EL}/η^p_{EL}	χ_s	Ref.
Pt monomer[b]	4.8	1.0	0.22 ± 0.01	5
CBP[c]		0.22	0.22 ± 0.02	30, 41
Alq_3[d]	2.7	0.56	0.22 ± 0.03	2

(b) Polymeric materials

(i) Direct comparisons of EL to PL

Material	η_{PL} (%)	$\eta_c\eta_{PL}$ (%)	η_{EL} (%)	η_{EL}/η_c (%)	γ	χ_s	Ref
OC1 C10-PPV[e]		8.5	4			>0.50	1
MEH-PPV[f]		8.5	1.3			>0.15	1
Green PPV[g]	33 ± 3		6 ± 0.5	23		>0.35–0.45	3
Orange PPV[h]	9 ± 1		1.8 ± 0.2	5.6		>0.35–0.45	3
MEH-PPV[i]		1.8	0.82		0.85 ± 0.15	0.20 ± 0.04	

(ii) Phosphorescent techniques

Material	η^f_{PL}/η^p_{PL}	η^f_{EL}/η^p_{EL}	χ_s	Ref
Pt polymer[j]	4.6	1.8	0.57 ± 0.04	5

singlet fractions of tris(8-hydroxyquinoline) aluminum (Alq3) = (20±1)%

singlet fractions of poly[2-methoxy-5-(2-ethylhexyloxy)-1,4-phenylenevinylene] (MEH-PPV) = (20±4)%.

M. Segal, M. A. Baldo, R. J. Holmes, S. R. Forrest, Z. G. Soos, Phys. Rev. B 68, 075211 (2003).

High EL efficiency

"Maximum EL efficiency of 24 cd/A were observed at 12 V, which corresponds to an external QE of 7.1%."

"We assume that triplet–triplet annihilation is responsible for this, in which triplet excited molecules, excitons, generated by carrier recombination, go through annihilative reactions with other triplet excited molecules to form singlet excited molecules [M. Pope and C. E. Swenberg, in *Electronic Processes in Organic Crystals* (Oxford University Press, New York, 1982), p. 64.] This process may be facilitated when a large number of excited molecules are generated at high bias voltages of over 10 V in this device."

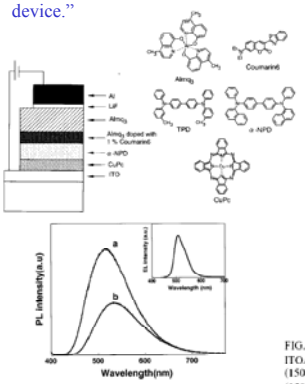

FIG. 2. Photoluminescence spectra of 1000-Å-thick vacuum evaporated films of (a) $Almq_3$ (λ_{ex}=395 nm) and (b) Alq$_3$ (λ_{ex}=395 nm). Inset: EL spectrum of an ITO (1000 Å)/CuPc (150 Å)/TPD (300 Å)/coumarin 6 (1%)-doped $Almq_3$ (150 Å)/$Almq_3$ (550 Å)/LiF (5 Å)/Al (1000 Å) device. Current density=25 mA/cm^2.

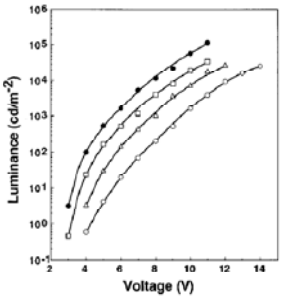

FIG. 3. Luminance–voltage characteristics of (open circles) ITO/TPD (300 Å)/$Almq_3$ (700 Å)/Mg:Ag, (open triangles) ITO/CuPc (150 Å)/TPD (300 Å)/$Almq_3$ (700 Å)/Mg:Ag, (open squares) ITO/CuPc (150 Å)/TPD(300 Å)/$Almq_3$ (700 Å)/LiF (5 Å)/Al (1000 Å), and (closed circles) ITO/CuPc (150 Å)/TPD (300 Å)/coumarin 6 (1%)-doped $Almq_3$ (150 Å)/$Almq_3$(550 Å)/LiF (5 Å)/Al (1000 Å) devices.

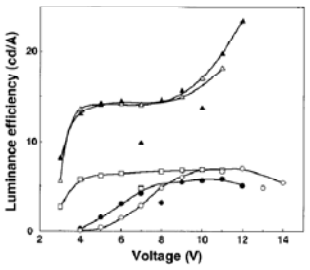

FIG. 4. EL efficiency–voltage characteristics of (open circles) ITO/TPD (300 Å)/$Almq_3$ (700 Å)/Mg:Ag, (closed circles) ITO/CuPc (150 Å)/TPD (300 Å)/$Almq_3$ (700 Å)/Mg:Ag, (open squares) ITO/CuPc (150 Å)/TPD (300 Å)/$Almq_3$ (700 Å)/LiF (5 Å)/Al (1000 Å), (open triangles) ITO/CuPc (150 Å)/TPD (300 Å)/coumarin 6 (1%)-doped $Almq_3$ (150 Å)/$Almq_3$ (550 Å)/LiF (5 Å)/Al(1000 Å), and (closed triangles) ITO/CuPc (150 Å)/α-NPD (400 Å)/coumarin 6-doped $Almq_3$ (150 Å)/$Almq_3$ (550 Å)/LiF (5 Å)/Al (1000 Å) devices.

Junji Kido and Yasuhiro Iizumi, Appl. Phys. Lett. 73, 2721 (1998)

How can we understand the result of $\eta_{EL} > 0.25\eta_{PL}$?

1. Small exciton binding energy → free e-h recombination.
2. Delayed fluorescence from the T-T annihilation (fusion).
3. Capture cross section of the singlet exciton is higher than that of the triplet exciton.

Triplet-Triplet Exciton Annihilation

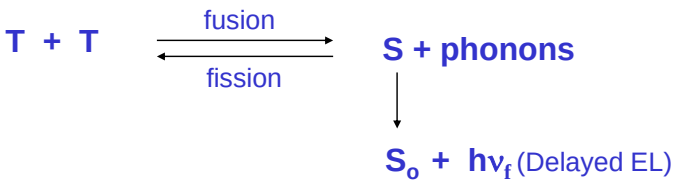

T + T → S* + So ; Spin 1 + 1 = 0, 1, 2

Singlet exciton : 1/9

Delayed Fluorescence

Intensity of the delayed fluorescence

$$I_{DF} = k_r[S_1] = \Phi_F \frac{1}{2} f\gamma_{tot}[T_1]^2$$

where kr is the rate constant for the radiative decay of the singlet states, $[S_1]$ is the density of the S_1 states, Φ_F is the quantum efficiency of the fluorescence, f is the fraction of the triplet-triplet annihilations that leads to a singlet exciton, γ_{tot} is the total bimolecular annihilation (fusion) rate constant, and the factor of 1/2 occurs since the disappearance of the two triplets results in only one singlet.

The time evolution of the concentration of the triplet state $[T_1]$ after the excitation light was turned off (t=0) is given by

$$\frac{d[T_1]}{dt} = -k_T[T_1] - \gamma_{tot}[T_1]^2$$

At very high triplet concentrations, $\frac{d[T_1]}{dt} \approx -\gamma_{tot}[T_1]^2 \Rightarrow [T_1]^{-1} \approx \gamma_{tot} t. \quad \therefore I_{DF}(t) \propto [T_1]^2 \propto \frac{1}{t^2}.$

After some time or by using a less-intense excitation light, the second term can be neglected due to the small triplet concentration ($k_T[T_1] >> \gamma_{tot}[T_1]^2$). The decay time of the DF intensity is half of the correlated triplet lifetime tT.

$$\frac{d[T_1]}{dt} \approx -k_T[T_1] \Rightarrow [T_1] \approx e^{-k_T t} = e^{-\frac{t}{\tau_T}} \quad \therefore I_{DF}(t) \propto [T_1]^2 \propto e^{-\frac{2t}{\tau_T}} = e^{-\frac{t}{\tau_{DF}}}.$$

M. Colle, C. Garditz, M. Braun, J. Appl. Phys. Lett. **96**, 6133 (2004)

Delayed Fluorescence in Alq3

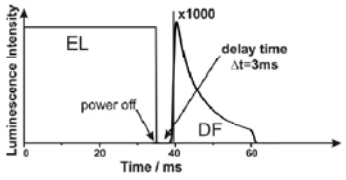

	τ_{DF}	$\tau_0(=2\tau_{DF})$	$\tau_{1/e}$	$\rho_{1/e}/\tau_{DF}$
α-Alq$_3$	6.6±0.5	13.2±1	13.6±0.5	2.05
Yellowish-green	7.8±0.5	15.6±1	16.2±0.5	2.08
δ-Alq$_3$	6.2±0.5	12.4±1	13.2±0.5	2.13
Film	4.33±0.5	8.66±1	9.3±0.5	2.15

M. Colle, C. Garditz, M. Braun, J. Appl. Phys. Lett. **96**, 6133 (2004)

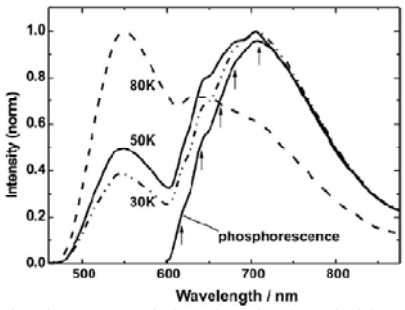

Delayed EL spectra of Alq3 taken after the end of the voltage pulse (Δt=3 ms) at 30, 50, and 80 K.

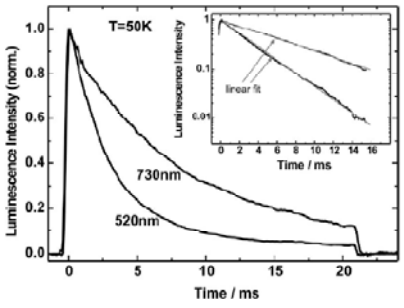

Transient intensity of the delayed luminescence detected at 520 and 730 nm, measured at a temperature of 50 K.

M. Colle and C. Garditz, Appl. Phys. Lett. **84**, 3160 (2004)

Triplet – Triplet (T – T) Annihilation

$$^3M^* + {}^3M^* \xrightarrow{k_{TT}^S} {}^1M^* + M, \qquad M + {}^1M^* \xrightarrow{\text{ISC}} M + {}^3M^*. \qquad {}^3M^* + {}^3M^* \xrightarrow{k_{TT}^T} {}^3M^* + M.$$

Rate equation for the triplet-triplet annihilation

$$\frac{dn_T}{dt} = -\frac{n_T}{\tau} - \frac{1}{2}k_T n_T{}^2 + \frac{J}{qd}$$

1) transient $\quad t > 0, J(t) = 0$

i) $k_T n_T(0) << \frac{1}{\tau} \qquad n_T \approx n_T(0)e^{-\frac{t}{\tau}}$

ii) $k_T n_T(0) >> \frac{1}{\tau} \qquad \frac{dn_T}{dt} \approx -k_T n_T{}^2$

$$n_T \approx \frac{1}{At+B} \qquad \frac{-A}{(At+B)^2} \approx \frac{-k_T}{(At+B)^2} \qquad \therefore A = \frac{1}{2}k_T, B = \frac{1}{n_T(0)}$$

$$\therefore n_T \approx \frac{1}{At+B} = \frac{1}{\frac{1}{2}k_T t + \frac{1}{n_T(0)}} = \frac{n_T(0)}{1+\frac{1}{2}n_T(0)k_T t}$$

Transient Solution

trial solution

$$n_T(t) = \frac{1}{Ae^{\frac{t}{\tau}} + B} \qquad \frac{-\frac{A}{\tau}e^{\frac{t}{\tau}}}{(Ae^{\frac{t}{\tau}}+B)^2} = -\frac{\frac{1}{\tau}}{(Ae^{\frac{t}{\tau}}+B)} - \frac{\frac{1}{2}k_T}{(Ae^{\frac{t}{\tau}}+B)^2}$$

$$-\frac{A}{\tau}e^{\frac{t}{\tau}} = -\frac{1}{\tau}(Ae^{\frac{t}{\tau}}+B) - \frac{1}{2}k_T \qquad \therefore B = -\frac{1}{2}k_T\tau$$

$$t = 0 \;;\; n_T(0) = \frac{1}{A+B} \qquad \therefore A = \frac{1}{n_T(0)} - B = \frac{1}{n_T(0)} + \frac{1}{2}k_T\tau$$

$$\therefore \quad n_T(t) = \frac{n_T(0)}{[1+\frac{1}{2}k_T\tau n_T(0)]e^{\frac{t}{\tau}} - \frac{1}{2}k_T\tau n_T(0)}$$

Light emission intensity $\quad L(t) = \frac{n_T(t)}{\tau} = \frac{L(0)}{(1+K\tau)e^{\frac{t}{\tau}} - K\tau} \qquad (let \;\; K = \frac{1}{2}k_T n_T(0))$

M. A. Baldo, C. Adachi, and S. R. Forrest, Phys. Rev. B 62,10967 (2000)

T – T Annihilation: Transient behavior

$$^3M^* + {}^3M^* \xrightarrow[\text{ISC}]{k_{TT}^S} {}^1M^* + M.$$
$$M + {}^1M^* \longrightarrow M + {}^3M^*.$$
$$^3M^* + {}^3M^* \xrightarrow{k_{TT}} {}^3M^* + M.$$

Rate equation for the T-T annihilation

$$\frac{dn_T}{dt} = -\frac{n_T}{\tau} - \frac{1}{2}k_T n_T^{\,2} + \frac{J}{qd}$$

Transient behavior: J=0

$$[^3M^*(t)] = \frac{[^3M^*(0)]}{\left(1 + [^3M^*(0)]\frac{k_{TT}\tau}{2}\right)e^{t/\tau} - [^3M^*(0)]\frac{k_{TT}\tau}{2}}$$

$$K = \tfrac{1}{2}k_{TT}[^3M^*(0)].$$

$$L(t) = \frac{L(0)}{(1+K\tau)e^{t/\tau} - K\tau},$$

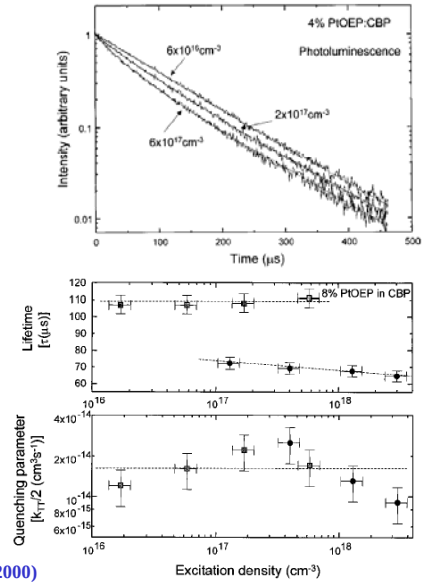

M. A. Baldo, C. Adachi, and S. R. Forrest, Phys. Rev. B 62,10967 (2000)

T – T Annihilation: Steady-state solution

$$\frac{dn_T}{dt} = 0 \qquad \frac{1}{2}k_T n_T^{\,2} + \frac{n_T}{\tau} - \frac{J}{gd} = 0$$

(근의 공식)

$$n_T = \frac{-\frac{1}{\tau} + \sqrt{(\frac{1}{\tau})^2 + \frac{2Jk_T}{qd}}}{k_T} = \frac{1}{k_T\tau}\left[-1 + \sqrt{1 + \frac{2Jk_T\tau^2}{qd}}\right] = \frac{1}{k_T\tau}\left[-1 + \sqrt{1 + \frac{8J}{J_T}}\right] \qquad (\because \frac{k_T\tau^2}{4qd} = J_T^{-1})$$

Light emission intensity $L = \frac{n_T}{\tau}$ **QE :** $\eta = \frac{L}{J} = \frac{n_T}{J\tau}$

η_0 : $k_T = 0$ 인 경우, 즉 , T-T annihilation이 없는 경우이므로 $\frac{n_T}{\tau} = \frac{J}{gd}$

$$\therefore \eta_0 = \frac{L}{J} = \frac{\frac{n_T}{\tau}}{J} = \frac{1}{qd}$$

$$\frac{\eta}{\eta_0} = \frac{qd}{k_T\tau^2 J}\left[-1 + \sqrt{1 + \frac{8J}{J_T}}\right] = \frac{J_T}{4J}\left[-1 + \sqrt{1 + \frac{8J}{J_T}}\right]$$

M. A. Baldo, C. Adachi, and S. R. Forrest, Phys. Rev. B 62,10967 (2000)

Efficiency Roll-off

Steady-State: d[^{3}M]/dt=0

$$\frac{\eta}{\eta_0}=\frac{J_0}{4J}\left(\sqrt{1+8\frac{J}{J_0}}-1\right), \qquad J_0=\frac{4qd}{k_{TT}\tau^2}$$

current density required to excite every phosphorescent molecule (i.e., the onset of saturation)

$$J_s=\frac{[M]qd}{\tau},$$

TABLE I. Current densities at the onset of T-T annihilation (J_0) as compared to predictions based on transient decays, and the estimated current density required to saturate the phosphors.

	1% PtOEP in CBP	1% PtOEP in Alq_3	8% PtOEP in CBP	8% PtOEP in Alq_3	16% PtOEP in CBP	16% PtOEP in Alq_3
J_0 from steady-state response (mA/cm^2)	0.8±0.1	2.4±0.2	4.4±0.4	3.8±0.4	4.4±0.4	7.4±0.7
J_0 from transient response (mA/cm^2)	7±2	8±3	5±2	5±2	4±1	6±2
Saturation threshold current density (mA/cm^2)	40±20	200±100	400±80	800±200	800±200	1000±300

M. A. Baldo, C. Adachi, and S. R. Forrest, Phys. Rev. B 62,10967 (2000)

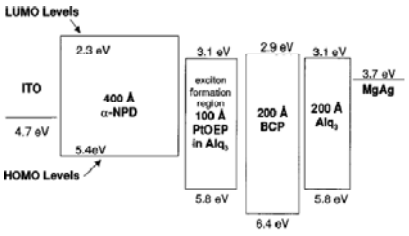

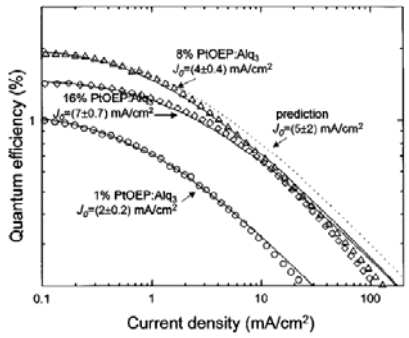

Triplet-polaron annihilation

$$\frac{d[^3M^*]}{dt}=-\frac{[^3M^*]}{\tau}-k_e[^3M^*][n_t]+\frac{J}{qd},$$

Assuming bulk limited transport, then [n_t] is proportional to the applied potential V,

$$\frac{\eta}{\eta_0}=\frac{1}{1+\alpha V},$$

$$J\propto V^{l+1}$$

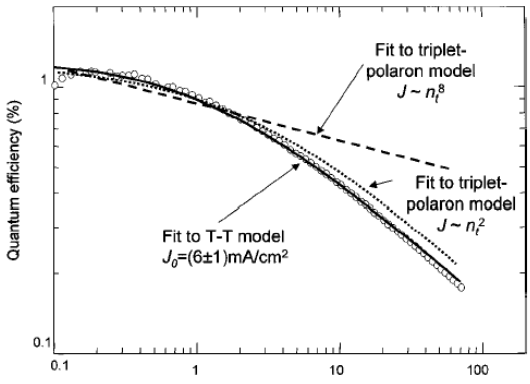

M. A. Baldo, C. Adachi, and S. R. Forrest, Phys. Rev. B 62,10967 (2000)

Triplet-polaron annihilation

$$\frac{d[n_{ex}]}{dt} = -\frac{[n_{ex}]}{\tau} - \frac{1}{2}k_{TT}[n_{ex}]^2 - k_P\left[\frac{\rho_c(j)}{e}\right][n_{ex}] + \frac{j}{ew}$$

$$\frac{\eta(j)}{\eta_0} = \Theta\left[\sqrt{\frac{\Delta^2 + \Gamma k_{TT}}{k_{TT}^2}} - \frac{\Delta}{k_{TT}}\right]$$

$$\Theta = \frac{ew}{\tau j},$$

	τ [μs]	k_{TT} [10^{-12} cm^3 s^{-1}]	$k_{P,e}$ [10^{-12} cm^3 s^{-1}]	$k_{P,h}$ [10^{-12} cm^3 s^{-1}]	η_0 [%]	w [nm]
TCTA:Ir(ppy)$_3$	(1.58±0.05)	(3±2)	(0.2±0.1)	(0.3±0.2)	15.8	10
NPB:Ir(piq)$_3$	(1.10±0.05)	(1.4±0.6)	(0.7±0.2)	(0.2±0.2)	7.6	19

$$\Delta \equiv \Delta(k_P) = \left(\frac{1}{\tau} + k_P C j^{1/(l+1)}\right)$$

$$\Gamma = \frac{2j}{ew}.$$

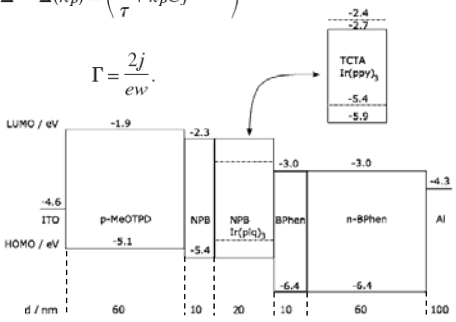

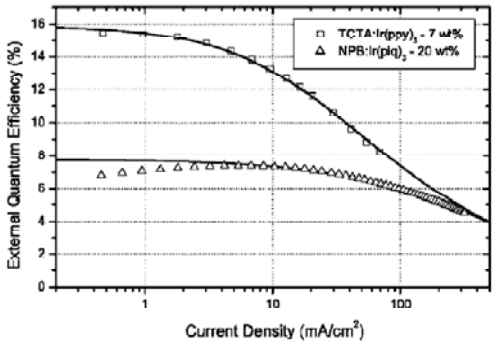

S. Reineke, K. Walzer, and K. Leo, Phys. Rev. B 75, 125328 (2007)